HHS Public Access

Author manuscript

Adv Mater. Author manuscript; available in PMC 2017 January 18.

Published in final edited form as:

Adv Mater. 2015 June 03; 27(21): 3285–3291. doi:10.1002/adma.201405634.

Co_9Se_8 Nanoplates as a New Theranostic Platform for Photoacoustic/Magnetic Resonance Dual-Modal-Imaging-Guided Chemo-Photothermal Combination Therapy

Xiao-Rong Song,
The Key Lab of Analysis and Detection Technology for Food Safety of the MOE, State Key Laboratory of Photocatalysis on Energy and Environment, College of Chemistry, Fuzhou University, Fuzhou 350108, PR China

Dr. Xiaoyong Wang,
State Key Laboratory of Molecular Vaccinology and Molecular Diagnostics, Center for Molecular Imaging and Translational Medicine, School of Public Health, Xiamen University, Xiamen 361005, PR China

Shu-Xian Yu,
The Key Lab of Analysis and Detection Technology for Food Safety of the MOE, State Key Laboratory of Photocatalysis on Energy and Environment, College of Chemistry, Fuzhou University, Fuzhou 350108, PR China

Jianbo Cao,
State Key Laboratory of Molecular Vaccinology and Molecular Diagnostics, Center for Molecular Imaging and Translational Medicine, School of Public Health, Xiamen University, Xiamen 361005, PR China

Shi-Hua Li,
The Key Lab of Analysis and Detection Technology for Food Safety of the MOE, State Key Laboratory of Photocatalysis on Energy and Environment, College of Chemistry, Fuzhou University, Fuzhou 350108, PR China

Dr. Juan Li,
The Key Lab of Analysis and Detection Technology for Food Safety of the MOE, State Key Laboratory of Photocatalysis on Energy and Environment, College of Chemistry, Fuzhou University, Fuzhou 350108, PR China

Gang Liu [Prof.],
State Key Laboratory of Molecular Vaccinology and Molecular Diagnostics, Center for Molecular Imaging and Translational Medicine, School of Public Health, Xiamen University, Xiamen 361005, PR China

Huang-Hao Yang [Prof.], and

Correspondence to: Gang Liu; Huang-Hao Yang.

X.R.S. and X.Y.W. contributed equally to this work.

Supporting Information

Supporting Information is available from the Wiley Online Library or from the author.

The Key Lab of Analysis and Detection Technology for Food Safety of the MOE, State Key Laboratory of Photocatalysis on Energy and Environment, College of Chemistry, Fuzhou University, Fuzhou 350108, PR China

Dr. Xiaoyuan Chen

Laboratory of Molecular Imaging and Nanomedicine (LOMIN), National Institute of Biomedical Imaging and Bioengineering (NIBIB), National Institutes of Health (NIH), MD 20892, USA

Theranostics is defined as the combination of diagnostic and therapeutic moieties into a single platform.[1] With the emergence of nanotechnology, theranostic nanoagents contribute significantly to the development of more effective and less toxic diagnostic and therapeutic interventions. Theranostics can allow us to simultaneously diagnose and treat diseases, track the agent's location, and evaluate the treatment efficacy. These nanoagents can also be customized by conjugation to biological ligands for targeting and can be used to develop multifunctional platforms for multimodal imaging and combination therapy.

In recent years, some theranostic nanoagents have been employed for cancer imaging and therapy, such as silica, carbon nanotubes,[3] polymeric nanoparticles,[4] gold-based nanostructures,[5] palladium-based composites,[6] magnetic nanoparticles[7] and lipid-based nanoparticles.[8] However, the scaffolds constructed by one diagnostic component and the other therapeutic components face enormous challenges, such as the inconsistency of the dose required for imaging and therapy.[9] Nanoagents that intrinsically have both diagnostic imaging and therapeutic capabilities have attracted much interest because they can avoid a complex synthetic process and improve patient outcome. Recently, benefiting from the distinct high specific surface areas, optical, thermal, and electronic properties, several kinds of 2D nanomaterials have served as powerful tools for theranostic applications, including reduced graphene,[10] transition metal dichalcogenides (TMDCs),[11] and topological insulators.[12] However, there are still great demands to develop new theranostic platforms for multimodal imaging-guided combination therapy to improve treatment efficacy.

Cobalt chalcogenides have emerged as promising non-noble metal-based nanoparticles in various applications, including lithium-ion batteries, cathode materials, and hydrogen evolution reaction catalyst.[13] Among these cobalt chalcogenides, cobalt selenides have attracted much attention due to their acid-stable property, optimal activity, as well as straightforward synthesis. Very recently, 2D cobalt selenides nanosheets were selectively synthesized and served as catalysts.[14] However, rare works have been done to study cobalt chalcogenides in biomedical application.

Here, we report the synthesis of biocompatible polyacrylic-acid-functionalized Co_9Se_8 nanoplates (PAA-Co_9Se_8 nanoplates) and then investigate their theranostic properties in vitro and in vivo for the first time (Figure 1a). We demonstrate that PAA-Co_9Se_8 nanoplates exhibit strong near-infrared (NIR) absorbance and low cytotoxicity. The NIR absorbance property is extensively applied to in vitro and in vivo photoacoustic imaging (PAI) and photothermal therapy (PTT) by 808 nm laser irradiation. Interestingly, PAA-Co_9Se_8 nanoplates can successfully serve as a T_2-weight magnetic resonance imaging (MRI) contrast agent to obtain good contrast enhancement in vivo. To the best of our knowledge,

the magnetic resonance signal enhancing capability of cobalt selenide was not reported before. Due to the high surface-area-to-mass ratio of 2D nanomaterials, PAA-Co_9Se_8 nanoplates can also be used as high drug loading nanocarriers to obtain PAA-Co_9Se_8-DOX complex, which shows pH-responsive chemotherapy. Furthermore, PAA-Co_9Se_8-DOX complex can be utilized for combined PTT and chemotherapy, which shows synergistic effect not only in in vitro cell culture assay, but also in a mouse tumor model. Clearly, PAA-Co_9Se_8 nanoplates are new powerful and promising theranostic nanoagents for biomedical applications.

Co_9Se_8 nanoplates were prepared according to Xie's method with minor modification.[14b] In order to make Co_9Se_8 nanoplates water-dispersible, we functionalized the surface with PAA by mixing the mixture of Co_9Se_8 nanoplates and PAA under sonication and then stirring in water. After removing the excess amount of PAA by centrifugation and washing three times with water, the PAA-Co_9Se_8 nanoplates solution with good water dispersibility was obtained. Atomic force microscopy (AFM) images revealed that most PAA-Co_9Se_8 nanoplates had a diameter of approximately 100 nm and a thickness of about 6 nm, suggesting that these nanoplates have a layered structure (Figure 1b, c). Dynamic light scattering (DLS) data and transmission electron microscopy (TEM) images also confirmed the size of PAA-Co_9Se_8 nanoplates was approximately 100 nm (Figure 1d and Figure S1, Supporting Information). The X-ray diffraction (XRD) pattern of the resulting products (Figure S2, Supporting Information) showed that all peaks could be identified as a cubic Co_9Se_8 structure, which is in agreement with the reported literature.[14b] After modifying the surface with PAA, the obtained PAA-Co_9Se_8 nanoplates were negatively charged with a zeta potential of −25 mV in aqueous solution (Figure S3, Supporting Information). The UV–vis–NIR absorbance spectrum was used to study the NIR absorbance properties of PAA-Co_9Se_8 nanoplates. As shown in Figure 1e, PAA-Co_9Se_8 nanoplates exhibited broad band absorbance in the NIR region.

In order to apply PAA-Co_9Se_8 nanoplates for biomedical use, the biocompatibility of nanomaterials is of primary concern. We used CCK-8 assay to evaluate the potential cytotoxicity of PAA-Co_9Se_8 nanoplates on HepG2 cancer cells. With the concentration of PAA-Co_9Se_8 ranging from 0 to 120 μg mL^{-1}, all of the cells retained over 90% viability. As shown in Figure 1f the cytotoxicity studies showed that PAA-Co_9Se_8 nanoplates possess low cell cytotoxicity and good biocompatibility.

Nanoparticles with strong NIR absorbance properties have attracted much interest in developing new theranostic platforms for biomedical imaging and therapy.[5,6,15] To investigate the photothermal performance, various concentrations of PAA-Co_9Se_8 nanoplates were exposed to a NIR laser (808 nm, 1 W cm^{-2}). With the increase of PAA-Co_9Se_8 nanoplates concentration or irradiation time, the temperatures of the aqueous solution containing PAA-Co_9Se_8 nanoplates increased accordingly (Figure 1g). Furthermore, the temperature of the solution containing 30 μg mL^{-1} of PAA-Co_9Se_8 nanoplates was elevated by ≈26 °C after laser irradiation for 10 min, while pure water increased only ≈3 °C under the same laser irradiation conditions. These good photothermal properties of PAA-Co_9Se_8 nanoplates motivated us to evaluate their potential for PAI and PTT.

PAI is an emerging technology formed by detecting the pressure wave caused by the photoacoustic effect.[5c,6b,16] Compared with other imaging modalities, PAI has several merits, such as high contrast, good spatial resolution, and reasonable penetration depth. Therefore, it makes great sense for us to develop new nanostructures for PAI. To demonstrate the capacity of PAA-Co_9Se_8 nanoplates as a new PAI contrast agent, we first evaluated the photoacoustic signals from aqueous solutions containing different concentrations of PAA-Co_9Se_8 nanoplates. As shown in Figure 2a,b, a higher photoacoustic signal was detected with increased concentrations of PAA-Co_9Se_8 nanoplates. We then investigated PAA-Co_9Se_8 nanoplates as a PAI contrast agent for cancer cell imaging. As expected, a brighter image was observed in cancer cells treated with PAA-Co_9Se_8 nanoplates than those without PAA-Co_9Se_8 nanoplates (Figure 2c).

Currently, multi-modal imaging tools, especially the combination of MRI and PAI, which provides not only volume imaging but also edge detection,[17] have made great contributions towards the development of more sensitive and accurate biological imaging systems. Because cobalt has three unpaired electrons and large saturation magnetization value (1422 emu cm^{-3}),[18] some zero-valence ferromagnetic cobalt particles based T_2-weight MRI contrast agents have been developed.[19] We subsequently investigated the potential of PAA-Co_9Se_8 nanoplates to enhance MRI contrast. As shown in Figure 2d, the darker MR images of the aqueous solution of PAA-Co_9Se_8 nanoplates were obtained as the concentrations of PAA-Co_9Se_8 nanoplates increased. The transverse relaxivity (r_2) of PAA-Co_9Se_8 nanoplates was determined to be 20.5×10^{-3} M^{-1} S^{-1} (Figure S4, Supporting Information). The negative enhancement in T_2-weight images indicated that PAA-Co_9Se_8 nanoplates could be a new MRI contrast agent. Although the T_2 relaxivity of Co_9Se_8 nanoplates now is relatively low, possibly due to their low saturation magnetization, the MRI contrast capability of Co_9Se_8 nanoplates may be further improved through morphology or dopant control.[20]

As a proof-of-concept experiment, we next utilized PAA-Co_9Se_8 nanoplates as a contrast agent for in vivo PAI/MRI dual-modal tumor imaging. All the animal experiments were carried out under protocols approved by Xiamen University Laboratory Animal Center. PAI was performed using an 808 nm laser as the excitation source before and after the injection of PAA-Co_9Se_8 nanoplates solution into HepG2 tumor-bearing mice. The PA images acquired after the injection of PAA-Co_9Se_8 nanoplates showed strong photoacoustic signals around the tumor region, while only major blood vessels could be seen without PAA-Co_9Se_8 nanoplates (Figure 2e). T_2-weight MR images were recorded before and after injection with PAA-Co_9Se_8 nanoplates with a 9.4 T MR instrument (Figure 2f). An obvious darkening effect at the tumor site could be observed after the injection of PAA-Co_9Se_8 nanoplates. The presented results confirmed that PAA-Co_9Se_8 nanoplates could be a promising dual-modal contrast agent for PAI and MRI.

Stimuli-responsive drug nanocarriers have recently attracted tremendous attention on account of their advantages,[21] such as high loading of anticancer drug, precise targeting to disease areas, and controllable drug release in response to special stimuli. In this work, we selected DOX as a model anti-cancer drug to investigate the drug loading and release with PAA-Co_9Se_8 nanoplates. After mixing the mixture of DOX and PAA-Co_9Se_8 nanoplates overnight, PAA-Co_9Se_8-DOX was obtained as precipitate through centrifugation. The UV–

vis– NIR absorbance spectrum of PAA-Co_9Se_8-DOX showed a characteristic DOX absorption peak at about 490 nm, which verified the successful loading of DOX onto PAA-Co_9Se_8 nanoplates (Figure 3a). PAA-Co_9Se_8-DOX showed a very weak fluorescence as compare with free DOX, which can suggest the strong binding of DOX to PAA-Co_9Se_8 nanoplates and effective fluorescence quenching by PAA-Co_9Se_8 nanoplates (Figure 3b). Furthermore, the loading efficiency of DOX on PAA-Co_9Se_8 nanoplates was improved in a DOX concentration-dependent manner (Figure 3c). The adsorption of DOX onto PAA-Co_9Se_8 nanoplates may be attributed to the hydrophobic interactions and the electrostatic interactions between DOX and the nanoplates.

To test the drug release profile, PAA-Co_9Se_8-DOX was dispersed in PBS at both pH 7.0 and 5.0. The release amount of DOX was calculated by determining the absorbance peak intensity at about 490 nm of the supernatant. As shown in Figure 3d, the release amount of DOX from PAA-Co_9Se_8-DOX at pH 7.0 was only 10% over 12 h, indicating the high stability of PAA-Co_9Se_8-DOX in biological media. However, 45% of DOX was released from PAA-Co_9Se_8-DOX at pH 5.0 over 12 h. These results may be caused by protonation of the amino group in the DOX molecule in an acidic solution, which weakens the hydrophobic interactions between DOX and PAA-Co_9Se_8 nanoplates. The pH-responsive drug release profile of PAA-Co_9Se_8 nanoplates was similar to other 2D nanocarriers reported previously.[22] It has also been reported that anticancer drugs can be released from NIR absorbable nanocarriers triggered by laser irradiation because the local hyperthermia could induce increased thermal vibration of polymer chains and weaken the interactions between the drugs and the nanocarriers.[23] We thus measured the DOX release profile with and without NIR laser irradiation for 5 min (808 nm, 1 W cm^{-2}). The data in Figure S5 (Supporting Information) revealed that the NIR irradiation can accelerate the release speed of DOX in the first two hours at pH 5.0. However, the DOX release speed and the release amount are slightly changed at pH 7.0 in spite of NIR irradiation. This phenomenon could be useful for NIR-triggered enhancement of intracellular drug release. Furthermore, the pH-dependent drug releasing properties could promote the drug release and accumulation at endo/lysosomal pH for effective chemotherapy.[24]

PTT employing photothermal conversion agent (PTCA) to convert NIR optical energy into thermal energy to kill cancer cells has been increasingly recognized as an effective and minimally invasive alternative to conventional approaches for cancer treatment.[3b,7c,17b,25] Inspired by the good photothermal property of PAA-Co_9Se_8 nanoplates, we first applied PAA-Co_9Se_8 nanoplates as a PTCA to cancer cell therapy. To verify the PTT effect, HepG2 cells treated with PAA-Co_9Se_8 nanoplates were stained with propidium iodide (PI) after NIR laser treatment. As shown in confocal laser scanning microscopy (CLSM) results (Figure S6, Supporting Information), the red fluorescence of PI increased with increased laser irradiation time, indicating the increase of cell death. Quantitative analysis of cell viability was then carried out after irradiating the cells with different concentrations of PAA-Co_9Se_8 nanoplates for 5 min. As shown in Figure 3e, cells with PAA-Co_9Se_8 nanoplates showed obviously lower cell viability under laser irradiation as compared with control experiments without laser irradiation. Moreover, cells incubated with 30 μg mL^{-1} of PAA-Co_9Se_8 nanoplates exhibited only 10% cell viability after NIR laser irradiation for 5 min, while almost 100% of cells remained alive without NIR laser irradiation. In addition, the cell

viability assay was examined after exposing the cells with same concentration of PAA-Co_9Se_8 nanoplates to laser for different lengths times (Figure S7, Supporting Information). These results revealed that PAA-Co_9Se_8 nanoplates are highly biocompatible and can be a potential PTCA for PTT of cancer.

We then quantitatively compared the difference of in vitro cytotoxicity between free DOX, PAA-Co_9Se_8 nanoplates, and PAA-Co_9Se_8-DOX complex with and without laser condition. Figure 3f showed that both free DOX and PAA-Co_9Se_8-DOX exhibited dose-dependent cytotoxicity. PAA-Co_9Se_8-DOX also showed relatively lower cytotoxicity than free DOX, likely because the gradual release of DOX from PAA-Co_9Se_8-DOX hindered the transport of DOX into cells and nuclei. However, it still holds great potential to develop pH-responsive drug nanocarriers, due to the fact that these nanocarriers not only can enhance the accumulation of the drug in tumor sites effectively but also allow multi-modal imaging and combination therapy to improve treatment efficacy. The results in Figure 3f clearly showed that PAA-Co_9Se_8-DOX had the most effective cell-killing effect in the presence of laser irradiation, presumably due to the combination of chemotherapy and photothermal heating. The combination therapy can obviously improve therapeutic effect and reduce drug dose, particularly when drug nanocarriers are applied to tumor elimination in vivo, where free drugs may be rapidly excreted.

Finally, in vivo antitumor experiments were carried out to suggest the combination of PTT and chemotherapy using PAA-Co_9Se_8-DOX. Tumor-bearing mice were prepared by subcutaneously injecting a suspension of 2×10^6 HepG2 cells in PBS (100 μL) into the back of the hind leg (6 weeks old, 20–25 g). In order to examine the in vivo photothermal effect of PAA-Co_9Se_8-DOX, an IR thermal camera was used to monitor the temperature change of the tumor areas before and after injection with PAACo_9Se_8-DOX (Figure 4a). As expected, tumors injected with PBS exhibited no significant temperature increase (≈37 °C) during 10 min of laser irradiation. The temperature of tumors injected with PAACo_9Se_8-DOX gradually increased with prolonged irradiation time and reached a plateau of ≈52 °C (Figure 4b), indicating the good photothermal performance of PAA-Co_9Se_8-DOX in vivo.

Tumor-bearing mice were then divided into four groups, i.e., control group, free DOX group, PAACo_9Se_8-DOX group, and PAA-Co_9Se_8-DOX plus NIR laser group. For tumor therapy, 100 μL of PBS, free DOX solution, or PAA-Co_9Se_8-DOX solutions (DOX 2.5 mg kg^{-1}, PAA-Co_9Se_8 nanoplates 5 mg kg^{-1}) were injected into tumors after the tumor sizes reached about 200 mm^3, and was followed by exposure to 808 nm laser at 0.75 W cm^{-2} for 10 min or no laser treatment. The body weights of the mice for all groups were measured during the treatments, and no significant weight loss was observed, indicating the low toxicity of all treatments (Figure 4c). As shown in Figure 4d and Figure S8, Supporting Information at 19 d after treatment the mice treated with free DOX, PAA-Co_9Se_8-DOX solutions, or PAA-Co_9Se_8-DOX plus NIR laser showed inhibition of tumor growth as compare with the control group. More importantly, the PAA-Co_9Se_8-DOX plus NIR laser group had almost complete tumor eradication, showing significantly enhanced therapeutic efficacy compared with other three groups. Hematoxylin and eosin staining of tumor slices (Figure 4e) revealed that tumor tissues in PAA-Co_9Se_8-DOX plus NIR laser groups showed more obvious necrosis and the tumor cells were more irregularly shaped with shrinking cell nucleus than that in free DOX

group and PAA-Co_9Se_8-DOX group. However, cancer cells in the control group retained regular cell morphology with intact cell nucleus. The significantly improved therapeutic efficacy of PAA-Co_9Se_8-DOX plus NIR laser treatment in vitro and in vivo could probably be attributed to a synergistic effect between PTT and chemotherapy. On one hand, NIR laser treatment can cause local hyperthermia to destroy most cancer cells and induce treated cells to be more susceptible to the damage caused by chemotherapy[26] On the other hand, the DOX release from PAA-Co_9Se_8 nanoplates can be stimulated by intracellular environment and can be accelerated by NIR laser irradiation to enhance chemotherapeutic efficacy. These results clearly confirmed that PAA-Co_9Se_8-DOX has potential applications for combined PTT and chemotherapy to receive superior therapeutic efficacy.

In summary, we successfully synthesized biocompatible PAA-Co_9Se_8 nanoplates and utilized them for in vitro and in vivo biomedical applications for the first time. The PAA-Co_9Se_8 nanoplates showed strong NIR absorbance, good photothermal performance, T_2 shortening effect, high drug loading capacity, as well as low cytotoxicity. We demonstrated that PAA-Co_9Se_8 nanoplates could be a promising contrast agent for PAI/MRI dual-modal imaging in vitro and in vivo. Furthermore, PAA-Co_9Se_8 nanoplates possess high drug loading capabilities for pH-responsive chemotherapy. We also proved that PAA-Co_9Se_8-DOX has the ability to combine chemotherapy with PTT to enhance cancer treatment efficacy. Although further studies, such as the function of tumor targeting and long-term toxicity, should be investigated before clinical translation, our work introduces a new theranostic nanoagent of PAA-Co_9Se_8-DOX for PAI/MRI-guided chemophotothermal combination therapy.

Experimental Section

Materials, details on synthesis of PAA-Co_9Se_8-DOX, and procedures for imaging and therapy methods are included in the Supporting Information.

Supplementary Material

Refer to Web version on PubMed Central for supplementary material.

Acknowledgments

The authors gratefully acknowledge the financial support from the National Basic Research Program of China (No. 2010CB732403, 2014CB744503), the National Natural Science Foundation of China (No. 21125524, 21475026, 81422023, 51273165), the Program for Changjiang Scholars and Innovative Research Team in University (No. IRT1116), the National Science Foundation of Fujian Province (No. 2010J06003), Program for New Century Excellent Talents in University (NCET-13– 0502), and Fundamental Research Funds for the Central Universities (2013121039).

References

1. a) Chen XY, Gambhir SS, Cheon J. Acc. Chem. Res. 2011; 10:841.b) Crawley N, Thompson M, Romaschin A. Anal. Chem. 2013; 86:130. [PubMed: 24313751] c) Janib SM, Moses AS, MacKay JA. Adv. Drug Delivery Rev. 2010; 11:1052.d) Muthu MS, Leong DT, Mei L, Feng SS. Theranostics. 2014; 4:660. [PubMed: 24723986]

2. a) Lee JE, Lee N, Kim T, Kim J, Hyeon T. Acc. Chem. Res. 2011; 10:893.b) Chen Y, Chen HR, Shi JL. Adv. Mater. 2013; 23:3144.c) Vivero-Escoto JL, Slowing II, Trewyn BG, Lin VS-Y. Small. 2010; 6:1952. [PubMed: 20690133]

3. a) Kostarelos K, Bianco A, Prato M. Nat. Nanotechnol. 2009; 4:627. [PubMed: 19809452] b) Kam NWS, Connell MO, Wisdom JA, Dai HJ. Proc. Natl. Acad. Sci. USA. 2005; 102:11600. [PubMed: 16087878] c) Liu Z, Liang XJ. Theranostics. 2012; 2:235. [PubMed: 22448193]

4. a) Duncan R. Cur. Opin. Biotechnol. 2011; 22:492.b) Kamaly N, Xiao Z, Valencia PM, Radovic-Moreno AF, Farokhzad OC. Chem. Soc. Rev. 2012; 41:2971. [PubMed: 22388185] c) Yang K, Xu H, Cheng L, Sun CY, Wang J, Liu Z. Adv. Mater. 2012; 24:5586. [PubMed: 22907876]

5. a) Xia YN, Li WY, Coley CM, Chen JY, Xia XH, Zhang Q, Yang MX, Cho EC, Brown PK. Acc. Chem. Res. 2011; 44:914. [PubMed: 21528889] b) Dreaden EC, Alkilany AM, Huang XH, Murphy CJ, El-Sayed MA. Chem. Soc. Rev. 2012; 7:2740.c) Huang P, Rong PF, Lin J, Li WW, Yan XF, Zhang MG, Nie LM, Liu G, Lu J, Wang W, Chen XY. J. Am. Chem. Soc. 2014; 136:8307. [PubMed: 24842342] d) Cheng K, Kothapalli S-R, Liu HG, Koh AL, Jokerst JV, Jiang H, Yang M, Li JB, Levi J, Wu JC, Gambhir SS, Cheng Z. J. Am. Chem. Soc. 2014; 136:3560. [PubMed: 24495038]

6. a) Huang XQ, Tang SH, Mu XL, Dai Y, Chen GX, Zhou ZY, Ruan FX, Yang ZL, Zheng NF. Nat. Nanotechnol. 2011; 6:28. [PubMed: 21131956] b) Chen M, Tang SH, Guo ZD, Wang XY, Mo SG, Huang XQ, Liu G, Zheng NF. Adv. Mater. 2014; 26:8210. [PubMed: 25363309]

7. a) Reddy LH, Arias JL, Nicolas J, Couvreur P. Chem. Rev. 2012; 112:5818. [PubMed: 23043508] b) Lin LS, Cong ZX, Cao JB, Ke KM, Peng QL, Gao JH, Yang HH, Liu G, Chen XY. ACS Nano. 2014; 4:3876.c) Tian QW, Hu JQ, Zhu YH, Zou RJ, Chen ZG, Yang SP, Li RW, Su QQ, Han Y, Liu XG. J. Am. Chem. Soc. 2013; 135:8571. [PubMed: 23687972]

8. a) Puri A, Blumenthal R. Acc. Chem. Res. 2011; 10:1071.b) Luk BT, Fang RH, Zhang LF. Theranostics. 2012; 12:1117.c) Ng KK, Lovell JF, Zheng G. Acc. Chem. Res. 2011; 44:1105. [PubMed: 21557543]

9. McCarthy JR. Nanomedicine. 2009; 7:693.

10. a) Liu Z, Robinson JT, Sun XM, Dai HJ. J. Am. Chem. Soc. 2008; 33:10876.b) Robinson JT, Tabakman SM, Liang Y, Wang H, Casalongue HS, Vinh D, Dai HJ. J. Am. Chem. Soc. 2011; 17:6825.c) Shen H, Zhang LM, Liu M, Zhang ZJ. Theranostics. 2012; 2:283. [PubMed: 22448195]

11. a) Chou SS, Kaehr B, Kim J, Foley BM, De M, Hopkins PE, Huang JX, Brinker CJ, Dravid VP. Angew. Chem. 2013; 125:4254.Angew. Chem. Int. Ed. 2013; 15:4160.b) Chhowalla M, Shin HS, Eda G, Li LJ, Loh KP, Zhang H. Nat. Chem. 2013; 5:263. [PubMed: 23511414] c) Cheng L, Liu JJ, Gu X, Gong H, Shi XZ, Liu T, Yong Y, Wang XY, Liu G, Xing HY, Bu WB, Sun BQ, Liu Z. Adv. Mater. 2014; 26:1886. [PubMed: 24375758] d) Chen ZG, Wang Q, Wang HL, Zhang LS, Song GS, Song LL, Hu JQ, Wang HZ, Liu JS, Zhu MF, Zhao DY. Adv. Mater. 2013; 25:2095. [PubMed: 23427112]

12. a) Zhang XD, Chen J, Min Y, Park GB, Shen X, Song SS, Sun YM, Wang H, Long W, Xie JP, Gao K, Zhang LF, Fan SJ, Fan FY, Jeong U. Adv. Funct. Mater. 2014; 12:1718.b) Li J, Jiang F, Yang B, Song XR, Liu Y, Yang HH, Cao DR, Shi WR, Chen GN. Sci. Rep. 2013:3.

13. a) Sidik RA, Anderson AB. J. Phys. Chem. B. 2006; 2:936.b) Yang ZJ, Lisiecki I, Walls M, Pileni MP. ACS Nano. 2013; 2:1342.c) Yin Y, Erdonmez CK, Cabot A, Hughes S, Alivisatos AP. Adv. Funct. Mater. 2006; 16:1389.d) Kong DS, Wang HT, Lu ZY, Cui Y. J. Am. Chem. Soc. 2014; 136:4897. [PubMed: 24628572]

14. a) Zhao JF, Song JM, Liu CC, Liu BH, Niu HL, Mao CJ, Zhang SY, Shen YH, Zhang ZP. CrystEngComm. 2011; 13:5681.b) Zhang XD, Zhang JJ, Zhao JY, Pan BC, Kong MG, Chen J, Xie Y. J. Am. Chem. Soc. 2012; 134:11908. [PubMed: 22779763]

15. a) Zhang ZJ, Wang J, Chen CY. Adv. Mater. 2013; 25:3869. [PubMed: 24048973] b) Shan G, Weissleder R, Hilderbrand SA. Theranostics. 2013; 3:267. [PubMed: 23606913] c) Min YZ, Li JM, Liu F, Yeow EKL, Xing BG. Angew. Chem. 2014; 126:1030.Angew. Chem. Int. Ed. 2014; 53:1012.d) Ke HT, Wang JR, Dai ZF, Jin YS, Qu EZ, Xing ZW, Guo CX, Yue XL, Liu JB. Angew. Chem. 2011; 123:3073.Angew. Chem. Int. Ed. 2011; 50:3017.

16. a) Wang LV, Hu S. Science. 2012; 335:1458. [PubMed: 22442475] b) De La Zerda A, Zavaleta C, Keren S, Vaithilingam S, Bodapati S, Liu Z, Levi J, Smith BR, Ma T-J, Oralkan O, Cheng Z, Chen XY, Dai HJ, Khuri-Yakub BT, Gambhir SS. Nat. Nanotechnol. 2008; 9:557.c) Pu K, Shuhendler

AJ, Jokerst JV, Mei JG, Gambhir SS, Bao ZN, Rao JH. Nat. Nanotechnol. 2014; 9:233. [PubMed: 24463363] d) Wilson KE, Bachawal SV, Tian L, Willmann JK. Theranostics. 2014; 4:1062. [PubMed: 25285161]

17. a) Kircher MF, De La Zerda A, Jokerst JV, Zavaleta CL, Kempen PJ, Mittra E, Pitter K, Huang RM, Campos C, Habte F, Sinclair R, Brennan CW, Mellinghoff IK, Holland EC, Gambhir SS. Nat. Med. 2012; 18:829. [PubMed: 22504484] b) Yu J, Yang C, Li J, Ding YC, Zhang L, Yousaf MZ, Lin J, Pang R, Wei LB, Xu LL, Sheng FG, Li CH, Li GJ, Zhao LY, Hou YL. Adv. Mater. 2014; 26:4114. [PubMed: 24677251]
18. Parkes LM, Hodgson R, Lu LT, Tung LD, Robinson I, Thanh NTK. Contrast Media Mol. Imaging. 2008; 3:150. [PubMed: 18756588]
19. a) Bouchard LS, Anwar MS, Liu GL, Hann B, Xie ZH, Gray JW, Wang XD, Pines A, Chen FF. Proc. Natl. Acad. Sci. USA. 2009; 106:4085. [PubMed: 19251659] b) Lukanov P, Anuganti VK, Krupskaya Y, Galibert AM, Soula B, Tilmaciu C, Velders AH, Klingeler R, Büchner B, Flahaut E. Adv. Funct. Mater. 2011; 21:3583.
20. a) Na HB, Song IC, Hyeon T. Adv. Mater. 2009; 21:2133.b) Zhao ZH, Zhou ZJ, Bao JF, Wang ZY, Hu J, Chi XQ, Ni KY, Wang RF, Chen XY, Chen Z, Gao JH. Nat. Commun. 2013; 4:2266. [PubMed: 23903002] c) Jang J-T, Nah H, Lee J-H, Moon SH, Kim MG, Cheon J. Angew. Chem. 2009; 121:1260.Angew. Chem. Int. Ed. 2009; 48:1234.
21. a) Mura S, Nicolas J, Couvreur P. Nat. Mater. 2013; 12:991. [PubMed: 24150417] b) Zhou L, Chen ZW, Dong K, Yin ML, Ren JS, Qu XG. Adv. Mater. 2014; 26:2424. [PubMed: 24347375] c) Tian JW, Ding L, Ju HX, Yang YC, Li XL, Shen Z, Zhu Z, Yu JS, Yang CJ. Angew. Chem. 2014; 126:9698.Angew. Chem. Int. Ed. 2014; 53:9544.d) Liu T, Wang C, Gu X, Gong H, Cheng L, Shi XZ, Feng LZ, Sun BQ, Liu Z. Adv. Mater. 2014; 26:3433. [PubMed: 24677423]
22. a) Lin LS, Cong ZX, Li J, Ke KM, Guo SS, Yang HH, Chen GN. J. Mater. Chem. B. 2014; 2:1031.b) Ma XX, Tao HT, Yang K, Feng LZ, Cheng L, Shi XZ, Li YG, Guo L, Liu Z. Nano Res. 2012; 3:199.c) Zhang W, Guo ZY, Huang DQ, Liu ZM, Guo X, Zhong HQ. Biomaterials. 2011; 32:8555. [PubMed: 21839507]
23. a) Park JH, von Maltzahn G, Ong LL, Centrone A, Hatton TA, Ruoslahti E, Bhatia SN, Sailor MJ. Adv. Mater. 2010; 22:880. [PubMed: 20217810] b) Wang C, Xu H, Liang C, Liu YM, Li ZW, Yang GB, Cheng L, Li YG, Liu Z. ACS Nano. 2013; 7:6782. [PubMed: 23822176] c) Yong Y, Zhou LJ, Gu ZJ, Yan L, Tian G, Zheng XP, Liu XD, Zhang X, Shi JX, Cong WS, Yin WY, Zhao YL. Nanoscale. 2014; 6:10394. [PubMed: 25047651]
24. a) Liu R, Zhang Y, Zhao X, Agarwal A, Mueller LJ, Feng PY. J. Am. Chem. Soc. 2010; 132:1500. [PubMed: 20085351] b) Liang K, Such GK, Johnston APR, Zhu ZY, Ejima H, Richardson JJ, Cui JW, Caruso F. Adv. Mater. 2014; 26:1901. [PubMed: 24375946] c) Zhao ZL, Meng HM, Wang NN, Donovan MJ, Fu T, You MX, Chen Z, Zhang XB, Tan WH. Angew. Chem. 2013; 125:7635.Angew. Chem. Int. Ed. 2013; 52:1.d) Lee ES, Kim D, Youn YS, Oh KT, Bae YH. Angew. Chem. 2008; 120:2452.Angew. Chem. Int. Ed. 2008; 47:2418.
25. a) Menon JU, Jadeja P, Tambe P, Vu K, Yuan B, Nguyen KT. Theranostics. 2013; 3:152. [PubMed: 23471164] b) Huang XH, EI-Sayed IH, Qian W, EI-Sayed MA. J. Am. Chem. Soc. 2006; 128:2115. [PubMed: 16464114] c) Hessel CM, Pattani VP, Rasch M, Panthani MG, Koo B, Tunnell JW, Korgel BA. Nano Lett. 2011; 11:2560. [PubMed: 21553924] d) Huang P, Lin J, Li WW, Rong PF, Wang Z, Wang SJ, Wang XP, Sun XL, Aronova M, Liu G, Leapman RD, Nie ZH, Chen XY. Angew. Chem. 2013; 125:14208.Angew. Chem. Int. Ed. 2013; 52:13958.
26. a) Pellicci PG, Dalton P, Orecchia R. Breast Cancer Res. 2011; 13:305. [PubMed: 21575278] b) Lee SM, Park H, Choi JW, Park YN, Yun CO, Yoo KH. Angew. Chem. 2011; 123:7723.Angew. Chem. Int. Ed. 2011; 50:7581.

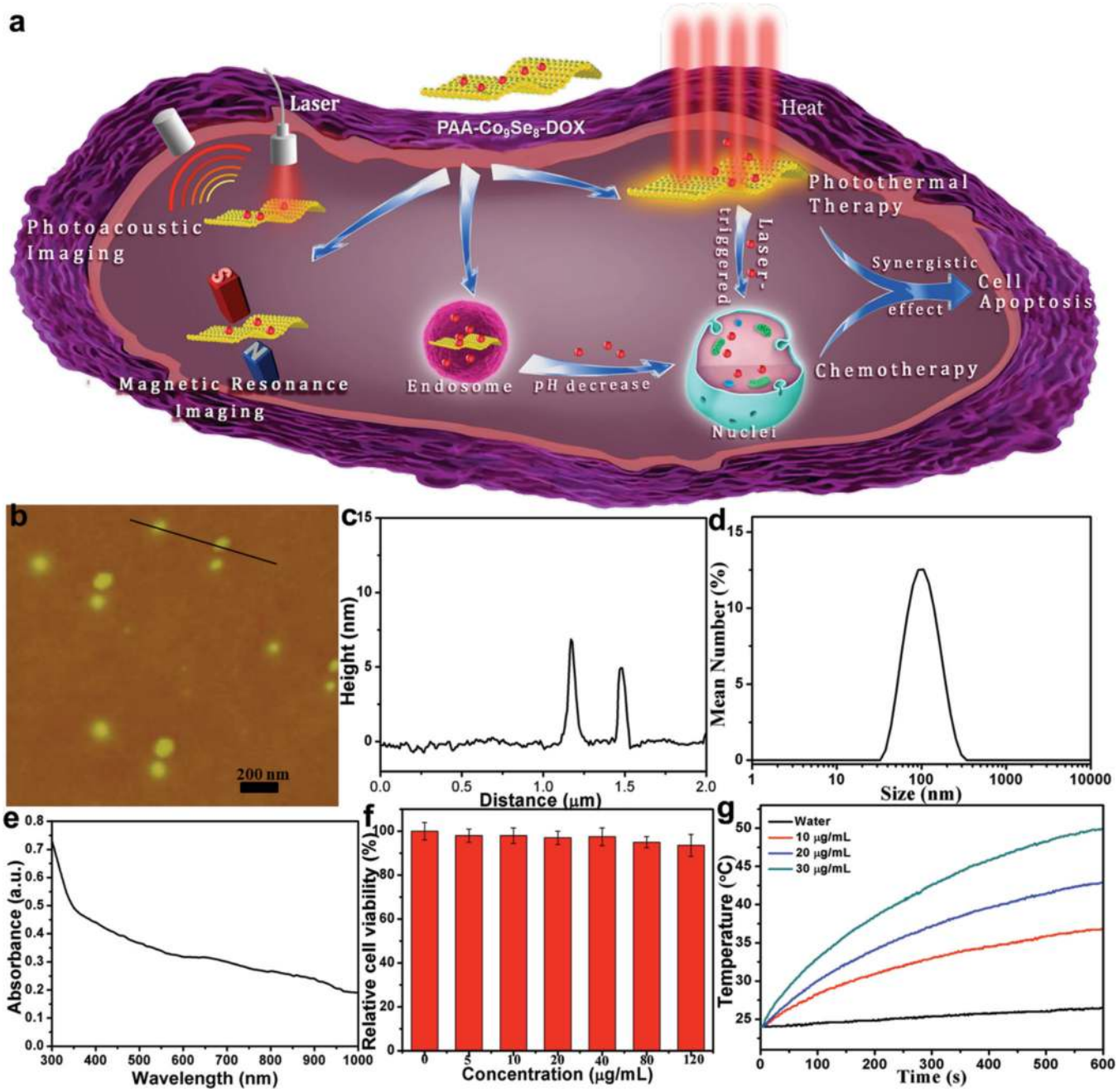

Figure 1.

a) Schematic illustration for the design of PAA-Co_9Se_8-DOX as a theranostic platform. b) AFM image of the synthetic PAA-Co_9Se_8 nanoplates. c) The corresponding height image of two random nanoplates. d) DLS measured sizes of as-synthesized PAA-Co_9Se_8 nanoplates in aqueous solutions. e) UV–vis–NIR absorption spectra of PAA-Co_9Se_8 nanoplates in water. f) Relative cell viability of HepG2 cells incubated with different concentrations of PAA-Co_9Se_8 nanoplates for 24 h. g) Temperature elevation of pure water and different concentrations of PAA-Co_9Se_8 nanoplates as a function of irradiation time.

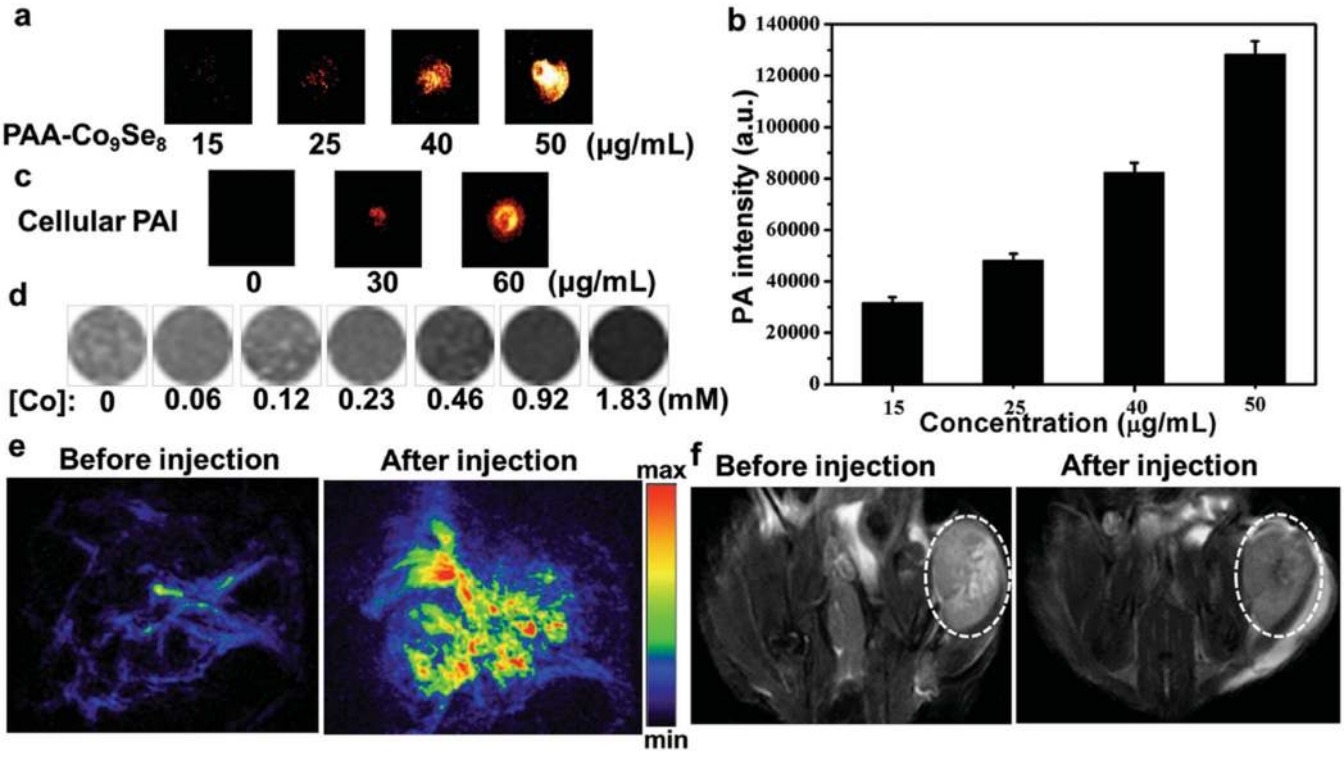

Figure 2.

a) PA images and b) PA intensity of aqueous dispersions contained different concentrations of PAA-Co_9Se_8 nanoplates. c) PA images of HepG2 cells (2×10^5) incubated with different concentrations of PAA-Co_9Se_8 nanoplates. d) T_2-weighted MR images of the PAA-Co_9Se_8 nanoplates in aqueous solution at different Co concentrations. e) PA images of tumor site before and after injection with PAA-Co_9Se_8 nanoplates. f) Representative T_2-weighted MRI scans of mice before and after injection with PAA-Co_9Se_8 nanoplates (the tumor areas are marked by the white circle).

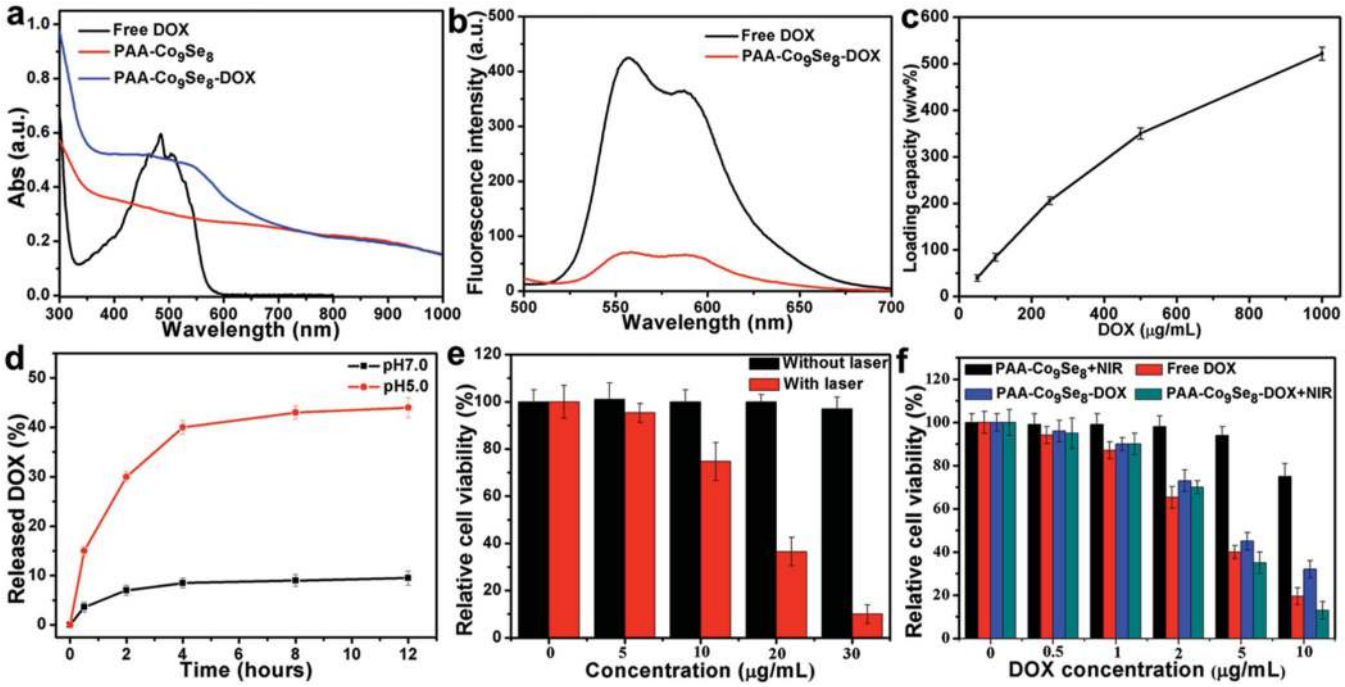

Figure 3.

a) UV–vis–NIR spectra of free DOX, PAA-Co_9Se_8 nanoplates and PAA-Co_9Se_8-DOX. b) Fluorescence spectra of free DOX and PAA-Co_9Se_8-DOX. c) DOX loading efficiency with different concentrations of DOX. d) DOX release profile of PAA-Co_9Se_8-DOX at different pH values. e) Cell viability of HepG2 cells exposed to different concentrations of PAA-Co_9Se_8 nanoplates with or without laser irradiation. f) Relative viability of HepG2 cells after various treatments.

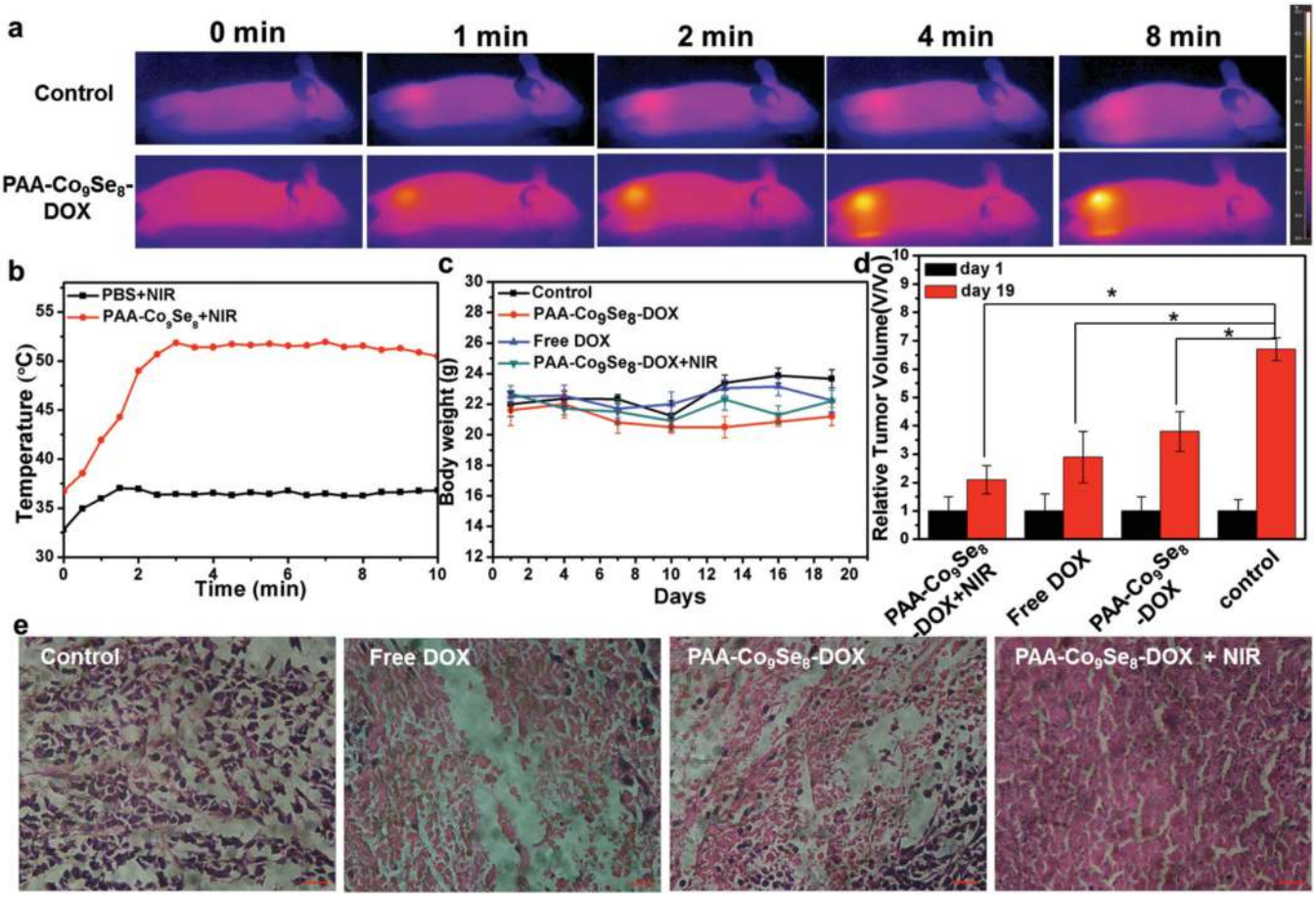

Figure 4.

a) IR thermal images of tumor-bearing mice after injection with PBS or PAA-Co_9Se_8-DOX exposed to the 808 nm laser at 0.75 W cm^{-2}. b) Tumor temperatures of mice monitored by the IR thermal camera as a function of the irradiation time. c) Body weights of mice in different groups. d) Relative tumor volume in different groups measured at the start and the end of various treatments. Asterisk indicates $P < 0.01$. e) Representative hematoxylin and eosin stained histological images from mice after various treatments.